Efficient organic solar cells by penetration of conjugated polymers into perylene pigments

doi: 10.1063/1.1804245

Efficient organic solar cells by penetration of conjugated polymers into perylene pigments

Jun-ichi Nakamura, Chiho Yokoe, and Kazuhiko Murata[a)]
E & I Materials Research Laboratory, Nippon Shokubai Co., Ltd., 5-8, Nishi Otabi-cho, Suita, Osaka 564-8512, Japan

Kohshin Takahashi
Division of Innovative Technology and Science, Graduate School of Natural Science and Technology, Kanazawa University, Kodatsuno, Kanazawa 920-8667, Japan

(Received 2 April 2004; accepted 13 August 2004)

We report here efficient air-stable *p-n* heterojunction organic solar cells with a structure consisting of an *n*-type insoluble perylene pigment penetrated by a *p*-type-conjugated polymer, where the interfacial area for photocurrent generation increases. The solar cells are easily produced by infiltrating a soluble-conjugated polymer intentionally into an opening among insoluble microcrystalline perylene layer under a saturated chloroform vapor. This approach can be regarded as an alternative convenient way to achieve bulk heterojunction solar cells. The cell performance is further enhanced by inserting an additional layer between the electrode and the photoactive layer to confine exciton in the photoactive layer. The overall attempt to improve the cell performance, so far, results in maximum quantum efficiency up to 45% under illumination of 485-nm monochromatic light and power conversion efficiency up to 1.9% under a simulated solar light (AM1.5) with a 100 mW cm^{-2} intensity. The approach is promising to achieve practical efficiency because tuning the opening size can further widen the photoactive area. © *2004 American Institute of Physics*. [DOI: 10.1063/1.1804245]

I. INTRODUCTION

Current progress for organic solar cells[1–9] from the standpoint of increasing power conversion efficiency is mainly attributed to the bulk heterojunction structure, which enables an efficient charge separation due to the increased photoactive interface area of *p-n* junction. The bulk heterojunction is typically attained by blending a *p*-type conjugated polymer and an *n*-type conjugated polymer[2] or a soluble C_{60} derivative,[3–8] resulting in up to 3.5% power conversion efficiency.[9] However, the corrosive top electrode, such as Ca, Al, and LiF, adopted in these cells brings a rapid decrease of the power conversion efficiency in atmospheric condition.

Endeavor to increase the power conversion efficiency of organic solar cells has been continued for more than decades though a practical level of efficiency has not been attained yet.[10–17] Achievement of a few percent of conversion efficiency is reported from several research groups recently.[2–5,8,9,18,19] The keyword for such achievement is "bulk heterojunction," namely widely spared photoactive *p-n* heterojunction interface that enhances the site of the photocharge generation and separation throughout the bulk. The bulk *p-n* heterojunction can be formed by blending soluble conjugated polymers,[2] mixing a low-molecular-weight organic compound into a conjugated polymer matrix,[3–9] or annealing vacuum-deposited organic compounds.[19] For example, Sariciftci *et al.* reported the solar cells based on the blend of an electron-donating conjugated polymer such as poly[2-methoxy-5-(3,7-dimethyloctyloxy)] - *p*-phenylene vinylene) (MDMO-PPV) or poly(3-hexylthiophene) (P3HT) and an electron-accepting soluble C_{60} derivative, [6,6]-phenyl C61-butyric acid methyl ester) (PCBM).[5,9] The power conversion efficiencies under simulated solar light (AM1.5) 80 mW cm^{-2} illumination for MDMO-PPV:PCBM blended cell and for P3HT:PCBM blended cell were 3.3% and 3.5%, respectively. In this case, a microphase separation occurred in the blended solid, creating the bulk heterojunction. While Peumans *et al.* prepared bulk heterojunction by annealing cells consisting of a codeposited *p*-type copper phthalocyanine and an *n*-type perylene pigment, yielding a power conversion efficiency of 1.5%.[19] The main issue for the previous bulk heterojunction cells arises from their corrosive top electrode such as Ca,[2] Al,[3] and LiF.[9] Due to the requirement of the corrosive top electrode, these cells must be prepared in an inert atmosphere or in a vacuum. Despite the elaborate cell preparation, the cell performance rapidly decreases after exposing it to air. To prevent the breakdown of the cell, it is necessary to seal the cell. Such sealing is difficult to be perfect for maintaining the long life of the cell and causes a significant costup canceling cost advantage of organic solar cells. It should be also noted that photocurrent which is originated from the photocorrosion of the corrosive electrode is sometimes mistaken as the energy-converted photocurrent.[20] We report here a fabrication method for bulk heterojunction cells with a noncorrosive Au top electrode having a remarkable stability in air without sealing.

II. EXPERIMENT

We use here a perylene pigment, (bisbenzimidazo[2,1-a:1′,2′-b′]anthera[2,1,9-def;6,5,10-d′e′f′]diisoquinoline-6,11-dione) (PV), which is well

a)Electronic mail: kazuhiko_murata@shokubai.co.jp

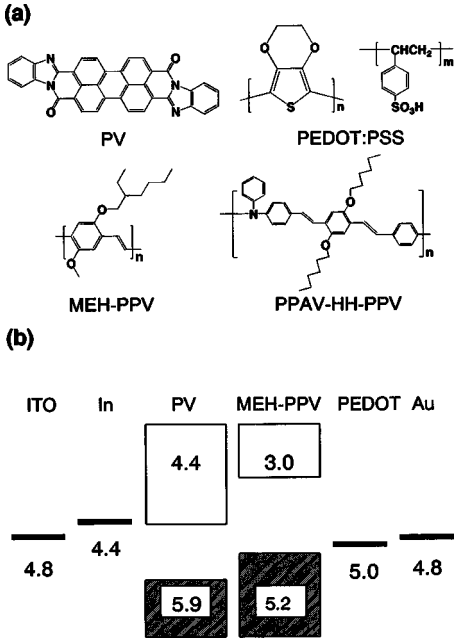

FIG. 1. Chemical structures, abbreviations, and the ionization potentials of the metal electrodes and the organic thin films. Chemical structures and abbreviations of the organic thin films in the solar cells (a). The ionization potentials of the metal electrodes and the organic thin films are measured by a Riken Keiki AC-2 photoelectron spectroscopy in air (b).

known as an *n*-type semiconductor,[15,21] whereas poly [2-methoxy-5- (2′-ethylhexyloxy)-1,4-phenylenevinylene] (MEH-PPV) and (poly(phenylimino-1,4-phenylene-1,2-ethenylene- 2,5-dihexyloxy-1,4-phenylene-1,2-ethenylene-1,4-phenylene) (PPAV-HH-PPV), both known as *p*-type semiconductors.[22,23] The chemical structures of their compounds were shown in Fig. 1(a). The PV and the PPAV-HH-PPV were synthesized and purified by literature methods.[24,25] The MEH-PPV purchased from the American Dye Source, Inc. and the poly(ethylenedioxy thiophene) doped with poly-(styrenesulfonic acid)(PEDOT:PSS) purchased from Aldrich were used without further purification. The molecular weight of the conjugated polymers was measured by a gel permeation chromatography (GPC) equipped with a Shodex KF-804L columns at 40 °C. The eluent was chloroform and the standard sample was polystyrenes.

The indium tin oxide (ITO)/ In/PV/conjugated polymer/ PEDOT/ Au sandwich-type cells were fabricated as follows. The In layer of 5-nm thickness was prepared onto a precleaned ITO electrode by a vacuum deposition at 3×10^{-5} Torr. The ITO electrode (sheet resistance: 8 $\Omega/\square$) was purchased from Merck Display Technologies Ltd. The PV was vacuum deposited at 3×10^{-5} Torr on the In layer. In the case of a standard cell preparation without the penetration treatment, about 0.4 wt% chloroform solution of MEH-PPV or PPAV-HH-PPV was spin coated on the insoluble PV solid film with a spin speed of 2000 rpm for 15 sec. Because chloroform rapidly evaporates in this case, a flat PPV layer was formed before penetrating into the PV layer. While in the case of the PPV penetration treatment, about 0.15 wt% of PPV chloroform solution was first dropped on the insoluble PV solid film, placed on a spin table, and left for 10 sec under a saturated chloroform atmosphere. Then, the table was gradually spun with linearly increasing the rotation speed from 0 to 2000 rpm for 40 sec still under a saturated chloroform atmosphere. Such chloroform treatment allows the PPV to have enough time to penetrate into the PV layer. Hence, whether the PPV penetrated into the PV layer or not simply depends on the evaporation time of the PPV chloroform solution. The PEDOT:PSS aqueous solution with a concentration of 1.3 wt% was spin coated at 8000 rpm on the PPV solid film and dried at 100 °C for 5 min under the vacuum of 3×10^{-5} Torr. Finally, a Au electrode of 25-nm film thickness was prepared on the PEDOT:PSS solid film by a vacuum deposition at 6×10^{-5} Torr. The geometric area of the solar cell was restricted to 0.04 cm^2.

The current-voltage curve of the solar cell was measured under the illumination of a simulated solar light (AM1.5) with 100 mW cm^{-2}, obtained by a Kansai Kagakukikai XES-502S.[26] The photocurrent action spectra were measured under the illumination of a standardized 15 μW cm^{-2} monochromatic light. In each measurement, the cells have been exposed to air and the illumination was carried out from the ITO side.

The thickness of the organic then films and their surface morphology were measured by a Digital Instrument Nano-Scope III a atomic force microscope (AFM). The thickness of the organic thin films was approximately 35 nm for the PV and 40 nm for the MEH-PPV and PPAV-HH-PPV. The absorption spectra of the organic films formed on a slide glass were recorded on a Shimadzu UV-3100 UV-visible spectrometer. The fluorescence spectra of the MEH-PPV solids on the Au and PEDOT:PSS/Au films formed on a slide glass were recorded on a Jasco FP-777 fluorescence spectrophotometer. The transmission electron microscopy (TEM) image of the cross section of the *p-n* heterojunction layer was measured by a Hitachi HF-2000 FE-TEM. As the TEM samples, PV, MEH-PPV, and Au layers were prepared on the polyethylene terephthalate (PET) film using the same method as the solar cells were prepared. Then, the multilayered film was crosscut with an interval of 100 nm. Namely, the TEM image was measured for the cross section of the film with a thickness of 100 nm. The ionization potentials of the metal electrodes and of the organic thin films were measured by a Riken Keiki AC-2 photoelectron spectroscopy in air.

For the measurement of the electrical conductivity for conjugated polymers, the Au/conjugated polymer/ Au surface-type cell was employed.[14] The interdigitated Au electrode, 0.15-mm wide and 207.7-mm long, was deposited on an alumina substrate. The organic solid film of about 50-nm thickness was spin coated on the Au electrode.

III. RESULTS AND DISCUSSION

The typical optimized cell structure in this work is the ITO/ In/PV/MEH-PPV or PPAV-HH-PPV PEDOT:PSS/Au. The In, PV, and Au are vacuum deposited, whereas the MEH-PPV, PPAV-HH-PPV, and PEDOT:PSS are fabricated by spin coating. The energy level of each material before contact, measured by the photoelectron spectroscopy, is illustrated in Fig. 1(b), indicating a suitable arrangement for

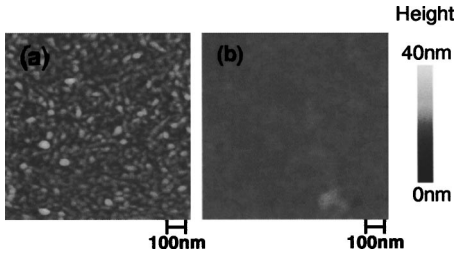

FIG. 2. AFM images of the solid film surface of PV (a) and MEH-PPV (b).

transporting the separated electrons and holes. The cells without In or PEDOT:PSS are also studied for comparison purpose.

Figure 2 shows the surface images of the vacuum-deposited PV solid film (a) and of the spin-coated MEH-PPV solid film (b) by an AFM. The PV surface has a small opening formed by microcrystalline PV particles of less than 20 nm. On the other hand, the MEH-PPV surface is amorphous and very smooth. From the AFM image, we thought of a fabrication way to increase the *p-n* heterojunction area, that is by penetrating PPV derivatives intentionally into the opening of the deposited insoluble PV layer by designing how to cast the soluble PPV derivatives, i.e., spin coated under an atmosphere of chloroform solvent.

The cell performances for both penetration-treated and nontreated PPV derivative/ PV *p-n* heterojunction cells with and without insertion of the additional electrode, In and PEDOT:PSS, are summarized in Table I. In fact, simple two-layer cells of the ITO/PV/MEH-PPV/ Au or ITO/PPAV-HH-PPV/ Au produced by the nontreated simple spin coating act as the *p-n* heterojunction solar cells with the energy conversion efficiency η of 0.40% and 0.33%, respectively, under illumination of a simulated solar light (AM1.5) with 100 mW cm^{-2}. All the cells given with the treatment of PPV penetration show a larger photocurrent, thus larger power conversion efficiency than the corresponding nontreated cells except the simple cell without insertion of the In or PEDOT:PSS. The reason that the increased photocurrent-generation area does not lead to an increase of the photocurrent in the ITO/PV/MEH-PPV/ Au cells is explained as follows. The penetrated MEH-PPV reaches to the ITO electrode where an ohmic contact is created, resulting in the back electron transfer of the photoproduced charge carriers from the ITO to the MEH-PPV, as shown in the energy diagram of Fig. 1(b).

By inserting a low-work-functional In layer with a thickness of 5 nm into the ITO/PV interface in both nontreated and penetration-treated PV/MEH-PPV cells, the short-circuit photocurrent J_{sc}, the open-circuit photovoltage V_{oc}, the fill factor *FF*, and consequently, the power conversion efficiency η increase from 0.40% to 0.78% in the nontreated cell and from 0.34% to 0.85% in the penetration-treated cell. This effect of In is accounted for assisting the ohmic contact between the ITO electrode and the *n*-type semiconductor PV with decreasing interfacial electrical resistance[27] and for prevention of the back electron transfer from the ITO electrode to the MEH-PPV.

According to the further insertion of PEDOT:PSS with a thickness of 50 nm into the MEH-PPV/ Au interface, in both nontreated and penetration-treated ITO/ In/PV/MEH-PPV/ Au cells, the η values of the cells improve from 0.78% to 0.98% in the nontreated cell and from 0.85% to 1.55% in the penetration-treated cell. To explain the effect of PEDOT:PSS on the increase of the photocurrent and efficiency, the photocurrent action spectra for the ITO/ In/PV/penetration-treated MEH-PPV/ Au cells with (○) and without (△) PEDOT:PSS layer are shown in Fig. 3 with the UV-visible (UV-VIS) spectra of the PV and MEH-PPV. In the ITO/ In/PV/penetration-treated MEH-PPV/ Au cell, the action spectrum follows only the absorption spectrum of the PV solid film, but does not reflect the absorption of the MEH-PPV film. While, the photocurrent action spectrum for the ITO/ In/PV/penetration-treated MEH-PPV/ PEDOT:PSS/Au cell approximately follows the sum of the

TABLE I. Performance of PV/conjugated polymer *p-n* heterojunction cells under a simulated solar light (AM1.5) with 100 mW cm^{-2} illumination.

Conjugated polymers	*d*(In)[a] (nm)	d(PEDOT)[b] (nm)	Penetration treatment[c]	*Jsc*[d] (mA cm^{-2})	*Voc*[e] (V)	*FF*[f]	η (%)[g]
MEH-PPV	0	0	No	2.44	0.56	0.29	0.40
	0	0	Yes	2.41	0.52	0.27	0.34
	5	0	No	2.84	0.65	0.42	0.78
	5	0	Yes	3.19	0.66	0.40	0.85
	5	50	No	3.22	0.62	0.49	0.98
	5	50	Yes	5.03	0.61	0.51	1.55
PPAV-HH-PPV	0	0	No	2.47	0.48	0.28	0.33
	5	50	No	4.15	0.64	0.50	1.34
	5	50	Yes	6.13	0.62	0.50	1.90

[a]Thickness of vacuum-deposited indium layer.
[b]Thickness of spin-coated PEDOT:PSS layer.
[c]Yes means the soluble PPV derivatives are intentionally penetrated into the opening of the vacuum-deposited PV layer. No indicates no penetration of the PPV derivatives is performed.
[d]Short-circuit photocurrent.
[e]Open-circuit photovoltage.
[f]Fill factor.
[g]Power conversion efficiency.

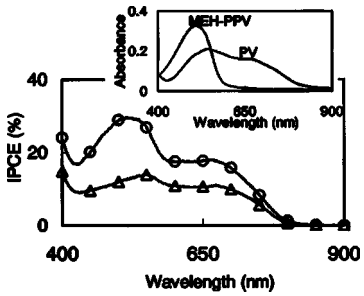

FIG. 3. Photocurrent action spectra of the PV/MEH-PPV *p-n* heterojunction solar cells under an illumination of a normalized 15 μW cm^{-2} monochromatic light. ○ represents the ITO/ In/PV/penetration-treated MEH-PPV/ PEDOT/ Au cell and △ represents the ITO/ In/PV/penetration-treated MEH-PPV/ Au cell. The inset shows the absorption spectra of the PV and MEH-PPV.

absorption spectra of the PV and MEH-PPV solids. Besides, it is experimentally proven that the fluorescence of the spin-coated MEH-PPV film on Au was completely quenched and was only slightly quenched when the PEDOT layer was inserted between the MEH-PPV and the Au. Hence, the photogenerated excitons that originated from the MEH-PPV solid effectively contribute to the photocurrent generation in the cell with PEDOT:PSS due to the exciton confinement by PEDOT:PSS. The results suggest that a diffusion length of MEH-PPV excitons is larger than 50 nm, the thickness of the MEH-PPV. This conclusion is not consistent with the previous results, where the exciton diffusion lengths of PPV are estimated as 7 ± 1 nm (Ref. 28) and 12 ± 3 nm.[29] If the effect of the exciton quenching by other layers can be eliminated, the diffusion length of PPV in the previously reported cells may increase, like in our case.

To prove the penetration of the PPV polymer into the PV layer, the TEM images for the cross section of the PET/PV/ (nontreated or penetration-treated) MEH-PPV/ Au are taken and shown in Fig. 4(a) and 4(b). The PV/nontreated MEH-PPV interface, produced by spin coating under an ambient atmosphere [Fig. 4(a)], is very smooth. The reason why the

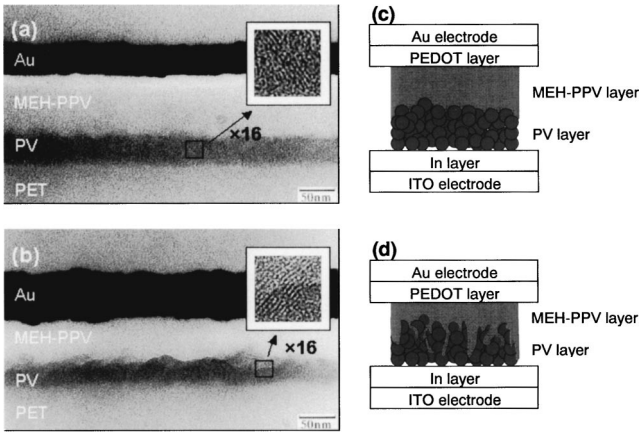

FIG. 4. TEM images of the cross section of the PET/PV/MEH-PPV/Au sandwich-type four-layer sheets produced by non (a) and penetration-(b) treated MEH-PPV. The amount of MEH-PPV in the PV/MEH-PPV film was kept constant for the both cells, confirmed by the absorption spectra of the PV/MEH-PPV film. The inset shows the 16 times expansion images for the selected areas. Model of the cross section of the solar cells produced by non (c) and penetration-(d) treated MEH-PPV.

surface roughness of ca. 20 nm for the PV according to the AFM is not visible here is explained as follows. If we can ideally observe the cross-section image without viewing the inside perpendicular to the cross section, the surface roughness of PV should be visible by TEM. To see the TEM image of the cross section, the sample needs to be crosscut as thin as possible, where the attainable minimum thickness is ca. 100 nm, which is much larger than the roughness of the PV layer.

Therefore, the TEM image of the 100 nm-thick sample is the superimposed view of the cross-section images within a depth of 100 nm; hence, the roughness of the PV layers are superimposed and disappeared apparently. On the other hand, the PV/penetration-treated MEH-PPV interface produced by spin coating in a saturated chloroform vapor [Fig. 4(b)] is wavy and the boundary is unclear. Because the crystal cross stripes of 1.4-nm width are observed in both PV layers regardless of the PPV penetration, as shown in the enlarged images, the PV keeps the crystal structure as it was without dissolution. Further, the thickness of the MEH-PPV in the nontreated cell appears to be about twice of that in the penetration-treated cell, despite that the thickness is intended by adjusting the experimental conditions and the VIS-absorption of both the PV/MEH-PPV films shows the same intensity. The apparent reduction of the MEH-PPV thickness after penetration is much more than can be accounted for by the penetration of the MEH-PPV into the PV. Due to the penetration, the top surface of the MEH-PPV layer turns to be rougher, affected by the rough interface between the MEH-PPV and the PV. As a result of that, the interface between the Au and the MEH-PPV has some roughness. When the rough Au/MEH-PPV interface is viewed by the TEM, it looks as if only the dark Au layer is superimposed. This means that the actual Au layer is thinner and the actual MEH-PPV is thicker than as observed by the TEM. The apparently thicker Au layer in Fig. 4(b) than in Fig. 4(a) supports it. The facts mentioned previously directly proved that the MEH-PPV infiltrated into the small opening formed by microcrystalline PV particles, creating large charge-separation area. The models of the cross section of the cells produced by the nonpenetration (c) and the penetration (d) of the MEH-PPV, are shown in Fig. 4. As illustrated in the figure, the photogenerated excitons smoothly migrate to the large charge-separation area through the connected PV particles and through the penetrated MEH-PPV solid; further photoproduced carriers with opposite charges are quickly transported from the *p-n* heterojunction interface to the cathode and anode, respectively. As a result of that, the MEH-PPV-penetrated cells therefore remarkably increased the photocurrent compared to the nonpenetrated cells. When the PPAV-HH-PPV is used instead of the MEH-PPV in the PPV-penetrated *p-n* heterojunction solar cell, the ITO/ In/PV/PPAV-HH-PPV(penetrated)/ PEDOT:PSS/Au cell shows a high η value of 1.9% under illumination of a simulated solar light (AM1.5) with 100 mW cm^{-2}, see Table I. This high value was derived from the high J_{sc} value of 6.13 mA cm^{-2}. The photocurrent-voltage ($J-V$) characteristics and an incident photon to current conversion efficiency (IPCE) spectrum for the ITO/ In/PV/PPAV-HH-PPV

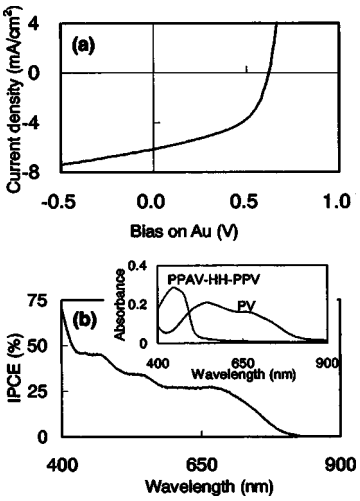

FIG. 5. Photocurrent–voltage characteristic (a) under illumination of a simulated solar light (AM1.5) with 100 mW cm^2, and photocurrent action spectra (b) under illumination of a normalized 15 μW cm^2 monochromatic light for the ITO/ In/PV/penetration-treated PPAV-HH-PPV/ PEDOT:PSS/Au *p-n* heterojunction solar cells. The inset shows the absorption spectra of the PV and PPAV-HH-PPV.

(penetrated)/ PEDOT:PSS/Au cell are shown in Fig. 5. The IPCE indicates 45% under illumination of the monochromatic light of 485 nm. This high value is attributed to the confinement of the excitons from the PPAV-HH-PPV, as explained before, but is not from an improvement of the electric conductivities, because it is measured that MEH-PPV (5×10^{-9} S cm^{-1}) is more conducting than PPAV-HH-PPV (3×10^{-11} S cm^{-1}). A GPC measurement showed that the weight-average molecular weight was 634 000 for MEH-PPV and 26 400 for PPAV-HH-PPV, respectively. Consequently, the viscosity of the PPAV-HH-PPV chloroform solution was much lower than that for the MEH-PPV. We assume that the PPAV-HH-PPV solution with lower viscosity penetrated easily into the nanoporous PV solid. After all, the contact area of the PV and the PPAV-HH-PPV, which is the photocurrent-generation site, seems to become larger than that of the PV and the MEH-PPV, affording a high J_{sc} value for the PV/PPAV-HH-PPV cell. However, we do not think that the increased photocurrent is attributed to this factor only, because by changing polymers, many more parameters than just viscosity change.

A noteworthy feature of our penetration-treated PPV solar cells is the air stability, on contrary to the previously reported PPV-based cells.[2–5] In the cell consisting of the blend of an electron-donating MEH-PPV and an electron-accepting poly[2,5-dihexyloxy-1,4-(1-cyanovinylene)phenylene] (CN-PPV) (Ref. 2) or in the cell consisting of the blend of an electron-donating MDMO-PPV and an electron-accepting fullerene derivative (PCBM),[4,5] the photocurrent is generated only when the photoactive layer is placed in the built-in potential gradient, which is created by two electrodes with different work function because the built-in potential gradient by the *p-n* heterojunction is compensated by such blending due to the isolation of the electron donor or acceptor from the electrode.[7,8] Therefore, the corrosive top electrode is typically required for these cells. Since direct connection of an *n*-type semiconducting layer (PV) to the bottom electrode and a *p*-type semiconducting layer (PPV derivatives) to the top electrode are still maintained in our cells, as shown in Fig. 4, the photocurrent is purely generated at the *p-n* heterojunction without the aid of the built-in potential by the two electrodes. In fact, even in a PV/MEH-PPV cell sandwiched by the ITO (4.8 eV) and Au(4.8 eV) with the same work function, the photocurrent is generated, as shown in Table I. The advantage that we can use the noncorrosive top electrode leads to the air-stable cells. Preliminarily, an experiment to check the durability of our cells shows that an ITO/ In/PV/penetration-treated MEH-PPV/ PEDOT:PSS/Au cell indicated no degradation of the cell performance after keeping the nonsealed cell for 60 days in air atmosphere. The cell also shows no decrease of the cell performance for 1 h under an illumination of a simulated solar light (AM1.5) with 100 mW cm^{-2} even though the MEH-PPV itself rapidly decompose and fades under the sun. The results indicate that when each photoactive layer is energetically well arranged and the electrons are transferred smoothly, side reactions leading to the degradation of the cell components hardly occur. This fact is promising to attain practically durable organic solar cells. The devolution of the photocurrent with longer illumination time is being studied.

IV. CONCLUSIONS

Organic solar cells with *p-n* bulk heterojunction, where PPV polymers are penetrated into nanoporous PV, were produced by spin-coating the soluble PPV onto insoluble PV film consisting of microcrystalline particles under a saturated chloroform vapor. Further ITO and Au electrodes were modified with In and PEDOT:PSS, respectively, leading to a more smooth electron transport and a utilization of the wide range of absorption by exciton confinement. Thus, the photovoltaic properties of the solar cells produced by the combination of those methods have been remarkably improved. We believe that this penetration cell is promising to give a low-cost and highly efficient organic solar cell in the near future, because the investigation for this kind of cell just started thus, a variety of further improvement is possible, for example, adjusting the porosity of; the PV, etc.

ACKNOWLEDGMENTS

The authors are deeply indebted to Dr. K. Yase, Dr. K. Saito, Dr. N. Tanigaki, and Dr. Y. Yoshida (National Institute of Advanced Industrial Science and Technology) for their helpful discussion. This work was partially supported by the New Energy and Industrial Technology Development Organization (NEDO) under the Ministry of Economy, Trade and Industry (METI).

[1]P. Peumans, A. Yakimov, and S. R. Forrest, J. Appl. Phys. **93**, 3693 (2003).
[2]J. J. M. Halls, C. A. Waish, N. C. Greenham, E. A. Marseglia, R. H. Friend, S. C. Moratti, and A. B. Holmes, Nature (London) **376**, 498 (1995).
[3]G. Yu, J. Gao, J. Hummelen, F. Wudl, and A. J. Heeger, Science **270**, 1789 (1995).
[4]S. E. Shaheen, C. J. Brabec, and N. S. Sariciftci, Appl. Phys. Lett. **78**, 841 (2001).
[5]C. J. Brabec, S. E. Shaheen, C. Winder, and N. S. Sariciftci, Appl. Phys.

Lett. **80**, 1288 (2002).
[6]V. D. Mihailetchi, P. W. M. Blom, J. C. Hummelen, and M. T. Rispens, J. Appl. Phys. **94**, 6849 (2003).
[7]T. Martens, *et al.*, Synth. Met. **138**, 243 (2003).
[8]M. Wienk, J. Kroon, W. Verhees, J. Knol, J. Hummelen, P. Van Hal, and R. Janssen, Angew. Chem., Int. Ed. **42**, 3371 (2003).
[9]F. Padinger, R. S. Rittberger, and N. S. Sariciftci, Adv. Funct. Mater. **13**, 85 (2003).
[10]F. Fan and L. R. Faulkner, J. Chem. Phys. **69**, 3334 (1978).
[11]R. O. Loutfy and J. H. Sharp, J. Chem. Phys. **71**, 1211 (1979).
[12]F. J. Kampas, K. Yamashita, and J. Fajer, Nature (London) **284**, 40 (1980).
[13]K. Takahashi, H. Nanbu, T. Komura, and K. Murata, Chem. Lett. **22**, 613 (1993).
[14]K. Takahashi, J. Nakamura, T. Yamaguchi, T. Komura, S. Ito, and K. Murata, J. Phys. Chem. B **101**, 991 (1997).
[15]C. W. Tang, Appl. Phys. Lett. **48**, 183 (1986).
[16]K. Murata, S. Ito, K. Takahashi, and B. M. Hoffman, Appl. Phys. Lett. **68**, 427 (1996).
[17]K. Takahashi, N. Kuraya, T. Yamaguchi, T. Komura, K. Murata, Sol. Energy Mater. Sol. Cells **61**, 403 (2000).
[18]M. Granström, K. Petritsch, A. C. Arias, A. Lux, M. R. Andersson, and R. H. Friend, Nature (London) **395**, 257 (1998).
[19]P. Peumans, U. Soichi, and S. R. Forrest, Nature (London) **425**, 158 (2003).
[20]K. Murata, S. Ito, K. Takahashi, and B. M. Hoffman, Appl. Phys. Lett. **71**, 67 (1997).
[21]G. Horowitz, F. Kouki, P. Spearman, D. Fichou, C. Nogues, X. Pan, and F. Garnier, Adv. Mater. 8, 242 (1996).
[22]A. J. Breeze, A. Salomon, D. S. Ginley, and B. A. Gregg, Appl. Phys. Lett. **81**, 3085 (2002).
[23]A. C. Arango, L. R. Johnson, V. N. Bliznyuk, Z. Schlesinger, S. A. Carter, and H. Hörhold, Adv. Mater. 12, 1689 (2000).
[24]T. Maki and H. Hashimoto, Bull. Chem. Soc. Jpn. **25**, 411 (1952).
[25]H. Hörhold, H. Rost, A. Teuschel, W. Kreuder, and H. Spreitzer, Proc. SPIE **3148**, 139 (1997).
[26]K. Imoto, K. Takahashi, T. Yamaguchi, T. Komura, J. Nakamura, and K. Murata, Bull. Chem. Soc. Jpn. **76**, 2277 (2003).
[27]M. Hiramoto, K. Ihara, and M. Yokoyama, Jpn. J. Appl. Phys., Part 1 **34**, 3803 (1995).
[28]J. J. M. Halls, K. Picher, R. H. Friend, S. C. Moratti, and A. B. Holmes, Appl. Phys. Lett. **68**, 3120 (1996).
[29]T. Stübinger and W. Brütting, J. Appl. Phys. **90**, 3632 (2001).